MILLIMETER-WAVE MEASUREMENT

The millimeter-wavelength spectral band covers the frequency range 30 GHz (λ = 10 mm) to 300 GHz (λ = 1 mm). In the larger view, it can include a part of the submillimeter band: the extended range up to 1 THz (λ = 0.3 mm), which represents one of the least explored portions of the electromagnetic spectrum. The frontier between the millimeter–submillimeter region and the far-infrared region is arbitrary and variable. The distinction comes mainly from the detection techniques employed (coherent or incoherent detection). The millimeter spectrum is presented in Fig. 1.

In the microwave domain, the atmosphere is transparent to frequencies up to 40 GHz except for a weak water vapor absorption line at 22 GHz. However, in the millimeter domain, there are several strong absorption lines: (1) a large and complex set of oxygen lines around 55 GHz to 60 GHz, (2) a single oxygen line around 119 GHz, and (3) a water vapor line around 183 GHz (see Fig. 2). These specific frequencies are used for instance to measure the atmospheric content in several space atmospheric sunder programs. Above 300 GHz, several absorption lines exist, mainly due to the water vapor. The spectral region located in between these lines, currently called "windows," is decreasingly transparent when the frequency increases.

Millimeter waves offer a solution to the increasing demand in frequency allocation for telecommunication applications due to the low-frequency-band saturation and the requirement for higher data rates. Moreover, a high directivity can be obtained with small antennas associated with small sized circuits which become more easily integrable. Applications are numerous, ranging from mobile communications, local area networks, and collision avoidance radars to satellite communications, radio-astronomy, radio-altimetry, atmospheric sunder, biologic spectroscopy, security and robotics.

In the millimeter-wave range up to 325 GHz (J band), the equipment and methods of measurement have been extended from the microwave domain. The major problems in the millimeter field are due to the small size of the devices and the transmission line losses. Above 300 GHz, as an alternative, other equipment and methods of measurement, using a quasi-optic setup, have been developed or adapted from far-infrared techniques (dielectric waveguide cavity resonator, free-space methods).

MILLIMETER-WAVE AUTOMATIC NETWORK ANALYZER

The reader is invited to consult Electric Noise Measurement ***Electric noise measurement***.

As all other types of vectorial network analyzer (*VNA*), the millimeter-wave vectorial network analyzer (*MWVNA*) measures magnitudes and phases of scattering parameters (*S* parameters) of the device under test (*DUT*).

Main Types of MWVNA

Broadband Coaxial Systems. In this group, single or multiple synthesized sweeper network analyzers are commercially available (1). The single synthesized source systems perform S-parameter measurements up to 50 GHz using 2.4 mm coaxial accessories, and up to 67 GHz using 1.85 mm coaxial elements (V connectors). The multiple synthesized sources system may cover the 40 MHz to 110 GHz frequency range using 1 mm coaxial elements (W connectors).

Rectangular Waveguide Systems. These network analyzers perform *S*-parameter measurements in Q (33 GHz to 50 GHz), U (40 GHz to 60 GHz), V (50 GHz to 75 GHz), and W (75 GHz to 110 GHz), G (140 GHz to 220 GHz) and J (220 GHz to 325 GHz) frequency ranges; the rectangular waveguide standards are WR-22, WR-19, WR-15, WR-10, WR-5 and WR-3 respectively.

In the multiple-source network analyzer, one synthesized source provides the radiofrequency (*RF*) (stimulus) signal and the second provides the local oscillator (*LO*) signal. Figure 2 shows a simplified block diagram of this system common to all waveguide bands. This system consists of a conventional network analyzer, two microwave sources (RF and LO), and a pair of band-dependent millimeter-wave test set modules covering the frequency bands given above. The RF signal after amplification is routed to the Port 1 test set module for forward measurements (S_{11} and S_{21}) or to the Port 2 test set module for reverse measurements (S_{22} and S_{12}). Components in the millimeter-wave test set module provide frequency multiplication, signal separation to sample incident, reflected and transmitted signals, and the harmonic mixers to accomplish the intermediate frequency (*IF*) conversion (generally first IF) to some MHz (e.g., 20 MHz). The second source provides the LO for the four harmonic mixers. This LO source is set such that the millimeter-wave RF test signal frequency and the appropriate LO harmonic are offset by exactly the IF (e.g., 20 MHz). For instance, in the case of the HP8510C MWVNA (1) with V-band millimeter-wave test set modules, the frequency of the two microwave sources (RF and LO) can be expressed as follows:

$$\mathrm{RF} = \frac{F_{\mathrm{op}}}{4} \quad \text{and} \quad \mathrm{LO} = \frac{(F_{\mathrm{op}} + 20\,\mathrm{MHz})}{14}$$

where F_{op} is the operating frequency.

As compared with a single-source network analyzer (coaxial), the rectangular waveguide system has inherent drawbacks. Indeed the power of the RF signal injected to the DUT cannot be controlled due to the frequency multiplication. This power may be close to 0 dBm (1 mW on 50 W system) and may be more dependent on the frequency band. This feature may induce nonlinear phenomena (compression, distortion) when the DUT is an active device (transistor, amplifier, etc.). Moreover, reactive impedance of a rectangular waveguide below its cutoff frequency may allow instability of the active DUT.

Dynamic Range of Millimeter-Wave Vectorial Network Analyzer

Dynamic range, which is the key consideration in most measurement systems, relates to the ability of a receiver to accurately detect a signal over a large range of magnitude. The largest input signal is usually limited by compression

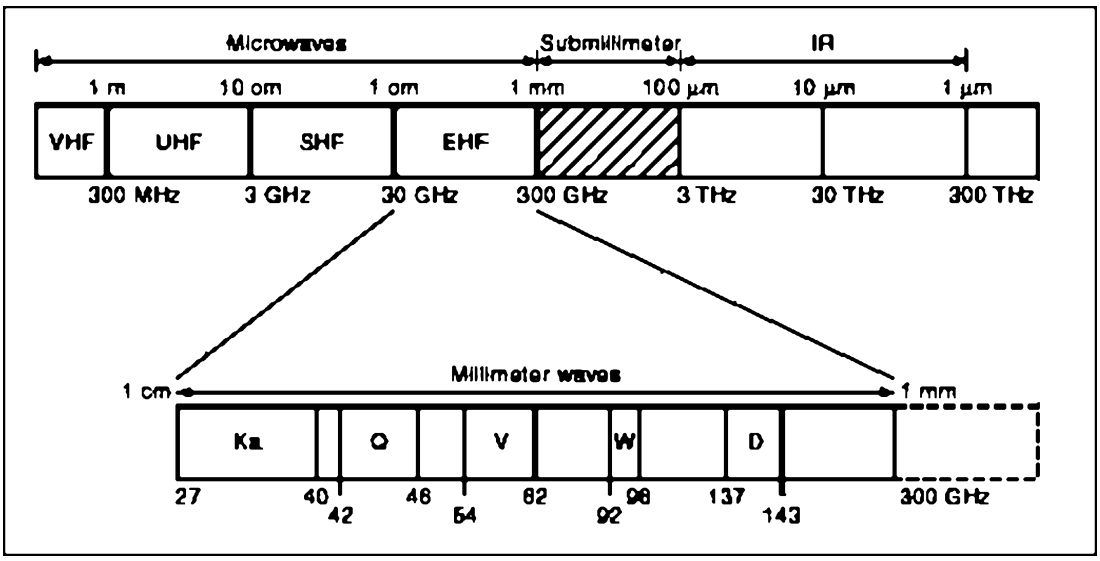

Figure 1. EM spectrum: definition of mm-wave frequency bands.

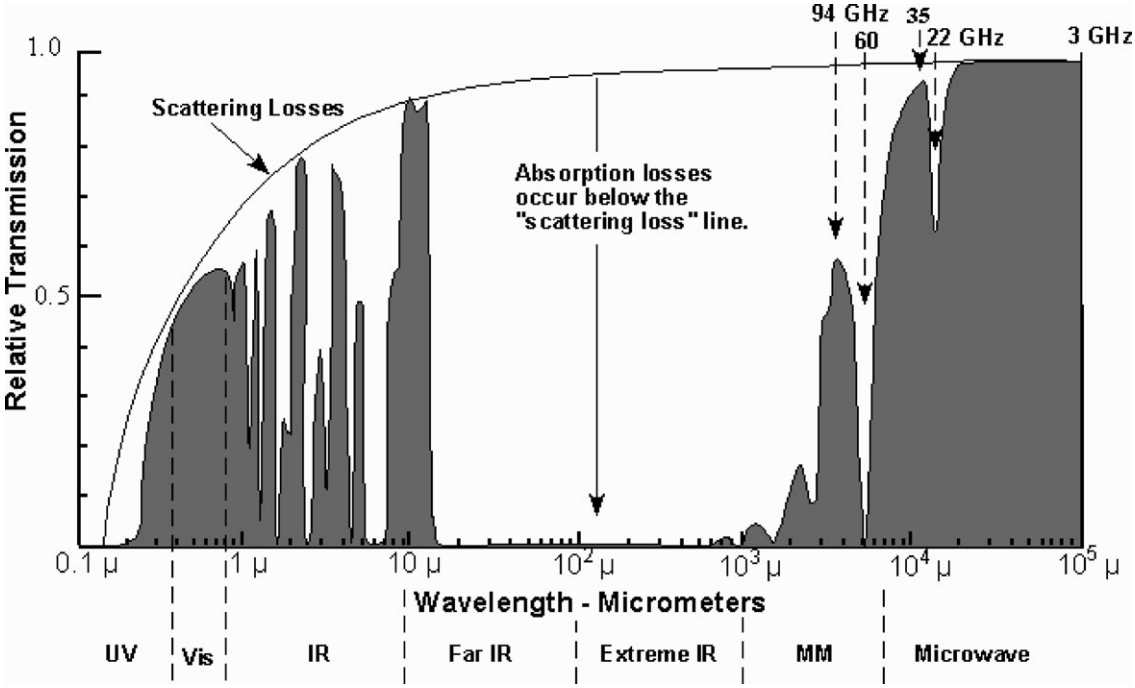

Figure 2. Atmospheric relative transmission of EM waves.

in the input receiver, while the smallest ones that can be detected are limited by the noise floor and other undesirable signals. Dynamic range can be improved by increasing the number of measurement averages and changing video IF bandwidth. Table 1 summarizes the dynamic range of PNA (®Agilent) network analyzer 110 GHz mm-wave system compared with 67 GHz PNA VNA (IF bandwith is 10 Hz). for transmission measurements as function of the frequency band.

High frequency probes

Commercially available coplanar probes cover the full millimeter-wave band (2). On-wafer probing in millimeter-wave measurement is by far the most precise technique, due to (1) better positioning and (2) better contact repeatability. For millimeter-wave measurement, only ground–signal–ground (*G–S–G*) topology is useful, since fundamental modes must only be excited at the probe tip. The microwave probes are constituted by: a connector (2.92, 2.4, 1.85 or 1mm) or a waveguide (WR-15 to WR-3) to connect the probe to the MWVNA and a micro coaxial line ended by three contacts (*G–S–G* coplanar configuration). There are mainly two types of coplanar probes: coaxial-to-coplanar probe tips and waveguide-to-coplanar probe tips. For the S-parameters measurement of active devices, the dc voltage and/or current are applied to the DUT through

System dynamic range (dB)	1.0 mm test port	1.85 mm PNA port
10 to 45 MHz	63	65
45 to 500 MHz	94	97
500 MHz to 2 GHz	120	123
2 to 10 GHz	116	123
10 to 24 GHz	111	121
24 to 30 GHz	100	112
30 to 40 GHz	92	107
40 to 45 GHz	84	101
45 to 50 GHz	85	103
50 to 60 GHz	80	100
60 to 67 GHz	70	95
67 to 70 GHz	68	n/a
70 to 75 GHz	74	n/a
75 to 80 GHz	85	n/a
80 to 100 GHz	89	n/a
100 to 110 GHz	87	n/a

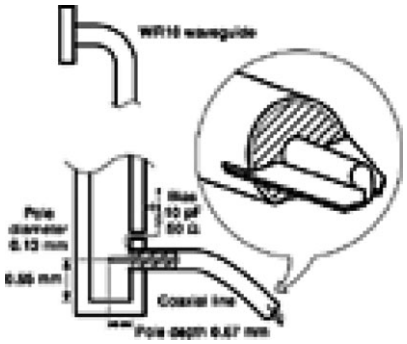

Figure 3. Mechanical structure of the waveguide–coaxial transition and the coaxial probe. (From Ref. 3.)

bias tees. In the case of coaxial system (cable and probe), we use the internal MWVNA test set bias tees generally, while waveguide probes may include a direct-current (*dc*) bias tee inside the probe (Fig. 3). Typical values for return loss and insertion loss are respectively, close to 15 dB and between 1 dB to 2 dB (2). The connection between the probe and the test set port must be kept as short as possible because and the millimeter-wave coaxial cable may easily add several decibels to the insertion loss.

Specific On-Wafer Calibration Technique

High-precision measurement relies on careful reference plane definition and on-chip parasitic access determination (4). Reference plane definition strongly correlates with the calibration used. For *SOLT* (short, open, load and through standards) calibration, the reference plane is defined by the coherent values declared for "short" and "open." Through losses must be kept low, and delay declaration must be coherent with reference plane positioning. Any inconsistency will lead to poor measurement. For *TRL* (through, reflect, line standards) or *LRM* (line, reflects, match standards) calibration, the reference plane is always located in the center of the through, but may be moved to some other convenient place after calibration. When using on-chip standards, some or all of the on-chip access parasitics may be included in the calibration, while use of specific standards (on alumina substrate) implies subsequent determination (deembedding) of the access parasitics. In the latter case, the reference plane is usually located under the probe tip. The main error sources are (1) bad calibration and (2) bad access parasitic determination. Advanced calibration techniques have been devised for improving calibration while use of specific on-wafer elements may improve deembedding of the access parasitic.

Advanced Calibration Technique. This technique uses more standards in order to (1) obtain better standards definition (SOLT calibration) and (2) perform vector errors correction (LRM calibration and TRL calibration). None of these techniques are implemented in ANA hardware, so specific computer programs are needed.

SOLT Enhancement. The reference plane is solely determined by the short declaration (usually 0 pH). An open-ended long line measurement is performed with an incorrect open declaration and an error model to allow finding for each frequency the open declaration error, thus leading to a better frequency dependent open declaration (5). This allows precise measurement with SOLT up to 110 GHz.

LRRM Calibration. A standard LRM calibration is performed, a new reflect is measured (a short if the calibration reflect was an open), and a new set of error vectors is calculated (6). This allows us to correct for small probe misplacement in addition to true load deviation.

NIST Multiline Calibration. The TRL calibration technique is based only on the accurate knowledge of the characteristic impedance of transmission line standards. One of the main drawbacks of TRL is its relatively narrow operating frequency range. To perform a very broadband (up to 110 GHz) TRL calibration, a multiline calibration technique has been proposed by the National Institute of Standards and Technology (*NIST*) (7).

Deembedding of the Access Parasitic

The use of an on-chip-specific design may allow precise determination of all access parasitics between a reference plane and a DUT port. This is an alternative to techniques

based on frequency dependence of Y and Z parameters which allow parasitic determination for transistor measurement (8). The deembedding uses direct S-parameter correction or correction through precise parasitic modeling using a specially designed on-chip test device.

Direct S-Parameter Correction. The measurement of open and short placed at the DUT port position allows direct S-parameter correction, using S to Y transformation:

$$Y_{\text{device}} = ((Y_{\text{meas}} - Y_{\text{open}})^{-1} - (Y_{\text{short}} - Y_{\text{open}})^{-1})^{-1}$$

This technique is frequently used for microwave measurement on silicon devices (CMOS or BiCMOS technologies) but is also interesting in millimeter-wave measurement. However, extreme care must be taken to compensate for open capacitance (fringing field) and short inductance (ground access) when designing the specific open and short device. These deembedding procedures do not take into account EM coupling with neighbor devices generally. Specific layouts with sufficient space between devices or devices separated by metallic shields are necessary.

Precise Parasitic Modeling. This usually uses several short, open, and through devices. A careful modeling of all these elements allows us to find out the true access parasitic and the intrinsic device parasitic. Once the access parasitic models are known, correction of the DUT measurement are obtained through the use of a linear simulator.

Specific Characterizations of Transistors in Millimeter Wave

In view of the increasing number of applications in the centimeter-wave range, the millimeter-wave range is now largely used. MVDS (40.5 GHz to 42.5 GHz), wireless local area networks (60 GHz WLAN, UWB), and automotive radar (77 GHz) are among the most focused millimeter-wave applications today. In addition, advanced technologies are now available for manufacturing integrated circuits used in this range. The main challenge is to design this integrated circuit accurately. To this end, reliable broadband transistor models are needed for designing a millimeter-wave integrated circuit. Linear models (or equivalent circuit) including high-frequency noise sources are usually deduced from S parameter and noise-parameter on-wafer measurements. The accuracy of each element of such models depends on the measurement accuracy. The determination of equivalent circuit elements may be difficult and inaccurate in the millimeter-wave range. The key considerations in designing a reliable equivalent circuit of transistors in the millimeter-wave range are as follows:

1. The choice of calibration technique as a function of the topology of the transistor and the nature of the substrate,
2. The choice of the equivalent circuit topology including parasitic elements.

Another solution consists in establishing an equivalent circuit of transistors from S parameters and noise parameters performed in a relatively lower frequency range (for instance, up to 50 GHz). The main advantage is that the accuracy of measurement in this frequency range is better controlled than that in the millimeter-wave range. To validate the reliability of such an equivalent circuit, we calculate the S parameters and noise parameters from the elements of the equivalent circuit and we compare these calculated data with measured ones in the millimeter-wave range.

Millimeter-Wave Cryogenic On-Wafer Measurement

There are basically two different solutions depending on the temperature range. For measurements down to 200 K, the setup is similar to that of the system used for high temperature measurement. The system works at ambient pressure, only the chuck is cold, and a local overpressure of drier air or nitrogen is used to prevent icing of wafer or probe tips. In this case, the temperature gradient is mainly located on the probe itself, so cable length at low temperatures is kept minimal. The calibration substrate may be kept at room temperature.

For measurements down to a few kelvin, the device and probes are kept under vacuum in a nitrogen or helium flow cryostat. Probe displacement under vacuum is obtained through the use of a bellow, cable length is significant, and calibration and measurement must be made at the same temperature.

VOLTAGE AND POWER RATIO TECHNIQUES: SIX-PORT NETWORK ANALYZER

The voltage and power ratio techniques and the six-port network analyzer (*SPNA*) are based on direct detection of the millimeter-wave. The hardware configuration of these measurement systems is simple because it is composed of diode or thermal detectors and of directional couplers or probes. In contrast, heterodyne detection systems involve multiple frequency conversions requiring local oscillators. The complexity of the measurement system makes random and systematic errors more difficult to estimate. That is why direct detection techniques provide much of the basis for precision microwave metrology. This article deals with the measurement of the scattering parameters S_{ij} of n-port millimeter devices using a slotted line, a (tuned) reflectometer, and an SPNA.

Slotted Line

This is the oldest method for measuring the reflection coefficient S_{11} of an impedance. In the millimeter frequency range, the slotted line is realized using a piece of metallic rectangular waveguide with a slot located at the center of the broad wall of the guide. The electric field inside the guide is sampled with a wire antenna connected to a Schottky diode detector. The magnitude of S_{11} is given by the voltage standing wave ratio (*VSWR*). The phase of S_{11} is given by the position of the antenna for which the detected voltage is minimum. This technique has been largely re-

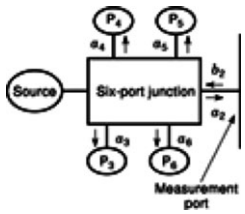

Figure 4. Six-port measurement system. It provides the complex value of the reflection coefficient S_{11} of the load connected at the measurement port. The power detector, connected at each output port, measures the power of b_i, where i = 3 to 6.

placed by an automated method.

The Tuned Reflectometer

A simple reflectometer requires one or two directional couplers and power detectors in order to measure the magnitude of S_{11}. These techniques suffer from low directivity of the couplers and from the mismatches of the source and the measurement port Γ_0. A tuned reflectometer includes tuners in order to overcome these difficulties. The measurement system is composed of a millimeter-wave source, one coupler of directivity D, one power detector, and two tuners. The detected power P may be written as follows:

$$P = K\left|\frac{S_{11} + D}{1 - S_{11}\Gamma_0}\right|^2$$

where K is a constant characterizing the measurement system.

The measurement procedure consists of successively connecting a sliding load and a sliding short in order to null D and Γ_0 using the tuners. Thereafter, the magnitude of S_{11} is given by the power ratio

$$|S_{11}| = \frac{P}{P_{cc}}$$

where P_{cc} is the power measurement when a short circuit takes place at the DUT. For a frequency equal to 110 GHz, the uncertainty measurement (defined at 2σ) of $|S_{11}|$ using the tuned reflectometer is in the range of 0.005 to 0.06 when $|S_{11}|$ varies from 0.01 to 0.5. In metrological labs, transmission measurements (S_{21}) are performed using an IF attenuator (IF substitution method).

Six-Port Network Analyzer

The name "six-port" is due to the six-port millimeter-wave junction (Fig. 4). At its four output ports it provides power readings P_3 to P_6 which are a weighted addition of the incident a_2 and reflected b_2 waves. The complex value of S_{11} (b_2/a_2) derives from the six-port equations:

$$\frac{P_i}{P_3} = K_i\left|\frac{\alpha_i a_2 + \beta_i b_2}{\alpha_3 a_2}\right|^2, \qquad i = 4, 5, 6$$

where α_i and β_i are the weighted factor of the waves a_2 and b_2 at the ith port and K_i is a constant of the power detector. The four scattering parameters may be obtained by the connection of two SPNAs at the two ports of the DUT or one SPNA in the reflection or transmission mode.

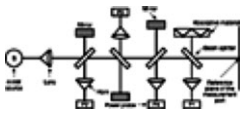

Figure 5. Six-port millimeter-wave junction using quasioptic techniques. It comprises five horns and four dielectric sheets. Each of the dielectric sheets is a beam splitter. A metallic mirror is placed on the fourth branch of each beam splitter except the one which involves the measurement of the source signal. The distance between the mirror and the dielectric sheet gives the weight of the added signals.

Practical SPNA Junctions

Six-port theory is, in principle, applicable to arbitrary design. However, for better accuracy assessment, design objectives should be obtained:

- At one output port, the wave is proportional (a_3) to the incident wave a_2.
- At the three remaining ports we have $|q_i| = 1.5$ and $\arg(q_i - q_j) = 120^\circ$, where $q_i = -\alpha_i/\beta_i$ for $i, j = 4, 5, 6$.

A simple six-port junction consists of one directional coupler and three voltage probes (as used in the slotted line) separated by about $\lambda/6$. A similar junction replaces the probes by a waveguide coupling structure (9). This structure contains two E-plane T junctions at the upper broad wall of the main R320 (26.5 GHz to 40 GHz) waveguide and one E-plane T junction at the lower broad wall. The distances between the T junctions are about $\lambda/6$.

Figure 5 shows a six-port junction using techniques (10) at sub-millimeter wave (300 GHz). Similar quasi-optical techniques have been applied in optic domains for a wavelength of 0.633 μm (11). The beam splitter may be replaced by directional couplers using a metallic waveguide or dielectric waveguide structure (94 GHz) (12).

A more wideband system (13) (75 GHz to 110 GHz) has been realized by means of connecting five 3 dB 90° hybrid couplers. It can be shown that the q_i points are frequency independent and are equal to $(-j, 1 + j, -1 + j)$ assuming identical and symmetrical couplers with a coupling factor of 3 dB. This feature is interesting in the millimeter-wave range because the phase property of commercial couplers are usually unknown.

Another technique is the multistate reflectometer. It consists of two directional couplers. The internal matched termination on the fourth arm of one coupler has been replaced by a phase shifter. Three states of the phase shifter provide the three equivalent power ratios of the six-port technique. Currently, this system permits on-wafer measurement at a frequency of 140 GHz (14).

Experimental Results

Table 2 shows S_{11} measurement results obtained with different systems. The measurement results labeled "SPNA," "HP8510," or "AB millimeter" can be compared with the values labeled "LCIE" given by the calibration center of *LNE* (Laboratoire National d'Essai en France), which are considered arbitrarily to be the references. In this case, the magnitude of S_{11} as determined with a tuned reflectometer

Table 2. Measurement Comparison Among Network Analyzers

Network Analyzer	93 GHz	94 GHz	95 GHz	96 GHz
LCIE	0.415	0.447	0.479	0.515
	100.8°	174.8°	91.4°	13°
SPNA	0.01	−0.013	0.012	−0.013
	−0.1°	+0.2°	−0.8°	7°
HP8510	0.005	0.002	0.01	0.002
	5°	3°	5°	3°
AB millimeter	0.006	−0.007	0.02	0.01
	0.1°	−4°	−3°	−1°

while the phase is obtained with a slotted line. The mean standard deviation is equal to 0.01 for the magnitude and 4° for the phase. The small differences may be due to temperature effects or the nonrepeatability of the connections.

Future Trends

The six-port junction may be realized using a microwave monolithic integrated circuit (*MMIC*)(15). The MMIC chips can be used as a sensor in an antenna array or integrated inside the tips of a probe station. In the latter case, the series of losses of the probe tips and the line connection do not decrease the measurement accuracy of the wafer probe station.

SOURCE-PULL AND LOAD-PULL TECHNIQUE

Large-signal millimeter-wave measurements of representative samples of semiconductor devices are of prime importance for two main reasons: accuracy and consistency check of nonlinear transistor models for CAD and experimental optimization of transistor optimum operating conditions without the use of any model.

Nonlinear devices demonstrate different aspects of their behavior depending on the source and load match. Therefore, large-signal measurement systems use either computer-controlled tuners or active loads to change source and load impedances of the DUT to reach the optimum matching conditions under large-signal operation (load-pull system).

Tuner systems operating up to the W band are commercially available. They are widely used for the design of low-noise amplifiers (16), power amplifiers (17), oscillators (18), and mixers (19). However, such systems do not allow synthesis of impedances close to the edge of the Smith chart because of inherent losses. This main drawback becomes more and more crucial if the operating frequency increases (millimeter wave) or if on-wafer measurements are performed. For these reasons the active source and load-pull technique has emerged. Active and passive source and load-pull techniques have their own advantages and suffer also from their own drawbacks. Going further in the large-signal characterization, novel measurement systems allowing the extraction of voltage/current waveforms at the DUT's ports have been developed.

Source and load-pull techniques—Frequency domain measurements

Passive load-pull technique. A block diagram of a passive load-pull system is given in figure 6. A systematic approach to perform large-signal characterization of a DUT is the following:

1. Impose desired DC voltages or currents
2. Tune the source and load networks
3. Sweep the power level of the source and measure powers, efficiency, and gain.

Then, the same procedure can be repeated for different operating conditions. This implies the use of a fully automated measurement system.

Basically, computer-controlled tuners are quite easy to implement in a large signal test-bed. Their linearity versus RF power level is obvious. This is an important feature for linearity characterization of devices under test using modulated RF signals like two-tone signals required for intermodulation measurements.

Furthermore as long as the tuners are connected very close to the DUT reference plane the synthesized impedances are almost the same over the whole bandwidth of the modulated RF signal. They are therefore quite similar to the source and load loci presented to the transistor under test when it is integrated in a MMIC.

Note that, when large signal source and load-pull measurements are performed under RF modulated signals a specific attention must be taken concerning low frequency impedances presented to the DUT by biasing circuits because envelope frequencies of the modulated signals are terminated into biasing circuits and may affect the DUT performances (20), (21).

The most accurate large signal characterization of a transistor is achieved if reflectometers are connected respectively between the source tuner and the input reference plane of the DUT and the output reference plane of the DUT and the load tuner. By connecting a VNA to these reflectometers AM/PM of the DUT can be measured. Furthermore accurate measurements of the input power really driving the nonlinear device under test can be done even if the nonlinear input impedance of the device varies versus RF power level. This is particularly crucial for highly mismatched power transistors.

Nevertheless in this situation, losses between the DUT and tuners are increased which is problematic for the syn-

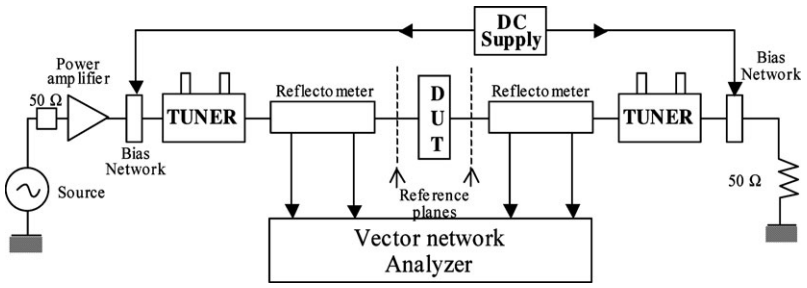

Figure 6. Passive load-pull system.

thesis of impedances having a high reflection coefficient in the millimeterwave domain. Waveguide reflectometers can be used to minimize losses. Unfortunately, they present high reflective impedances at low RF and microwave frequencies which can yield to DUT instability during measurements. The use of coaxial wave-probe reported in (22) may provide an attractive solution. In the microwave domain (f < 18 GHz), harmonic tuners are commercially available. They enable load impedance control at the first three harmonics. In the millimeter-wave domain, tuners enable nowadays only the control of impedances at the fundamental operating frequency.

Active load-pull technique. A block diagram of an active load-pull technique is given in figure 7 and has been reported in (23).

A source-pull implementation with a microwave six port junction is shown in figure 8 and has been reported in (24).

Depending on the position of switch 1, the input six-port measures either the input reflection coefficient of the DUT or the reflection coefficient of the source impedance presented to the DUT.

It is obvious that active load-pull techniques provide an attractive solution to overcome problems due to losses at microwaves. Nevertheless, two main problems may be encountered when using active loop techniques.

First, the loop amplifier must be oversized in order to remain in its linear region when the RF power driving the DUT is swept. This is particularly a key point if highly reflective impedances must be synthesized.

Second, special cares must be taken to avoid loop instabilities at frequencies different from the operating frequency.

I. Yattoun (25) has proposed enhanced solutions for that. But, the most important problem encountered using active loops is due to their inherent group delay which remains a drawback for the synthesis of representative impedance loci over the bandwidth of modulated signals when such signals are used for linearity characterization of the device.

Pulsed load-pull system. Either in active or passive load-pull systems, pulsed DC and RF signal configuration can be implemented. A block diagram is given in figure 9. It is mainly interesting to investigate the influence of thermal aspects instead of VNA in transistor performances.

Peak power meters can be connected to reflectometers shown in the block diagram sketched in figure 9. But VNA with pulsed capabilities need to be used if both AM/AM and AM/PM measurements of the DUT are required and if measurements of these parameters are wanted at the beginning, middle and end of the pulse duration. This kind of work has been reported in (26).

Waveform measurement system—Time domain measurements

Time domain waveform measurements require simultaneous measurements of fundamental and harmonic spectral components of microwave signals. Therefore, sampling scope techniques must be used instead of power meters or vector network analyzers. At microwave and millimeter wave, the best trade off between measurement speed, time base distorsion and dynamic range is reached by using harmonic sub-sampling techniques. The sub-sampling frequency is in the order of tens MHz. Equivalent time waveforms of microwave signals are obtained using samplers that perform a frequency translation and compression of microwave signals into an IF bandwidth as sketched in figure 10.

The COMB generator provide harmonics kf_S of a fundamental frequency f_S = 20 MHz which is the sub-sampling frequency. IF spectral components are digitized using a high dynamic range ADC.

The large signal network analyzer LSNA is a four channel instrument based on this harmonic sub-sampling principle. Each channel consists of a sampler, an IF filter and an ADC. The 4 measurement channels are fully synchronized.

The LSNA can be connected to a load-pull set-up as shown in figure 11.

The calibration of the system is performed in three main steps:

1. Classical TRL or LRRM calibration
2. Power calibration
3. Phase calibration

During this third step, a reference generator (step recovery diode) which provide harmonic spectral components with known phase relationships is connected to the reference plane of the DUT (27). The reference generator is calibrated using the nose-to-nose calibration procedure (28).

This set-up enables the extraction of voltage and current waveforms at the DUT reference planes.

It has been mainly used for large signal measurement based modeling purpose of nonlinear devices or for enhanced validation of nonlinear model of transistors for CAD (29), (30), (31), (32), (33).

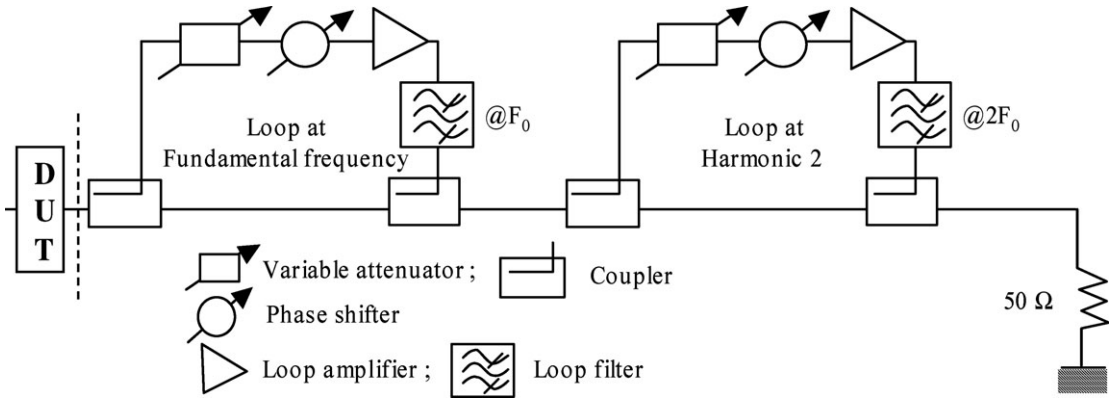

Figure 7. Active harmonic load-pull configuration.

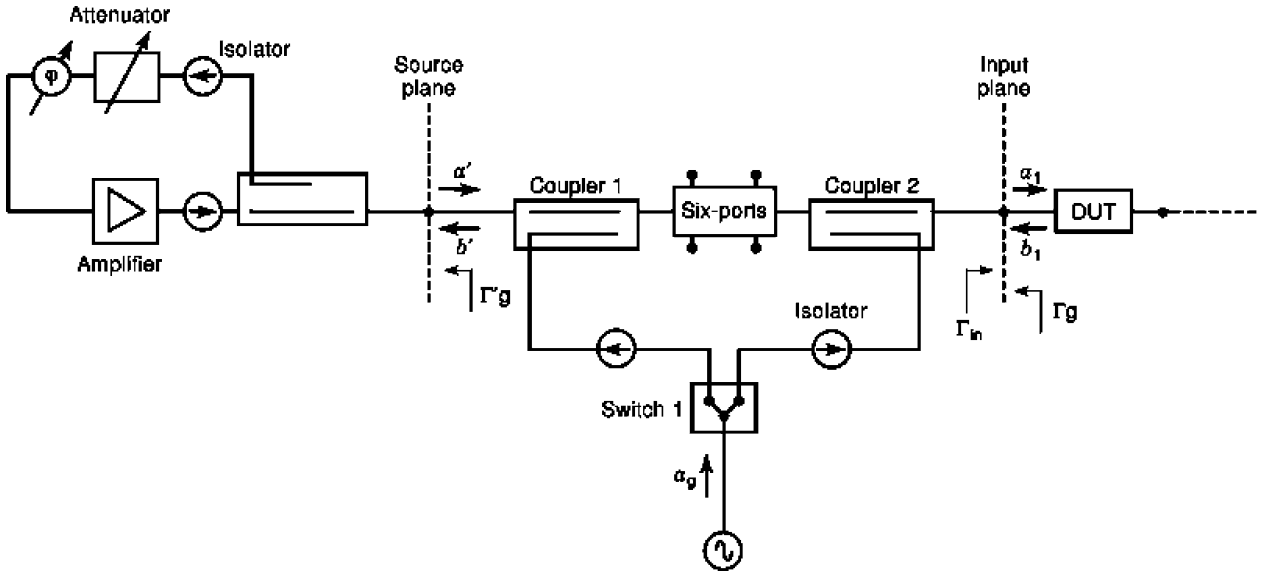

Figure 8. Source-pull implementation with a millimeter-wave six-port junction.

DIELECTRIC WAVEGUIDE CAVITY RESONATOR

At millimeter-waves, resonators are useful for a large number of applications in communication systems and measurements of dielectric properties. In the millimeter-wave and submillimeter-wave ranges, difficulties arise from wavelengths which are very short, and devices are difficult to machine with a large degree of accuracy. So the problem is to achieve high circuit Q for volumic or hybrid millimeter-wave integrated circuits.

Different resonator structures are used. Some of them are derived from low-frequency application, like a cylindrical metallic cavity, but other devices have been developed specially for millimeter-wave measurement. In the following subsections we present mainly the devices given in Fig. 12 which are often used.

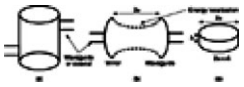

Figure 12. Example of millimeter-wave resonators. (a) Cylindrical metallic cavity. (b) Open resonators. (c) Whispering gallery dielectric resonators.

Cylindrical Metallic Cavity

This structure presented in Fig. 12(a) is composed of a cylindrical metallic waveguide closed at the top and the bottom by a metallic plane. The resonant frequency depends on the dimensions of the cavity (diameter and height) and the mode which is excited in the structures. These modes are chosen to be TE_{01n} or TM_{01n} modes and depend on excitation line position. The unloaded Q factor of these resonators increases with the axial number n. But it is difficult to use axial numbers greater than five, because a lot of modes are excited in a frequency band and it is difficult to obtain good frequency isolation. Typically, at room temperature and with copper to realize the cavity, values of unloaded Q factor are equal to 12,000 at 30 GHz and 7000 at 100 GHz on the TE_{013} modes.

Open Resonators

The most popular of this type of resonator is the Fabry–Pérot, which is presented in Fig. 12(b) (34, 35). These resonators are used from the short-microwave to the

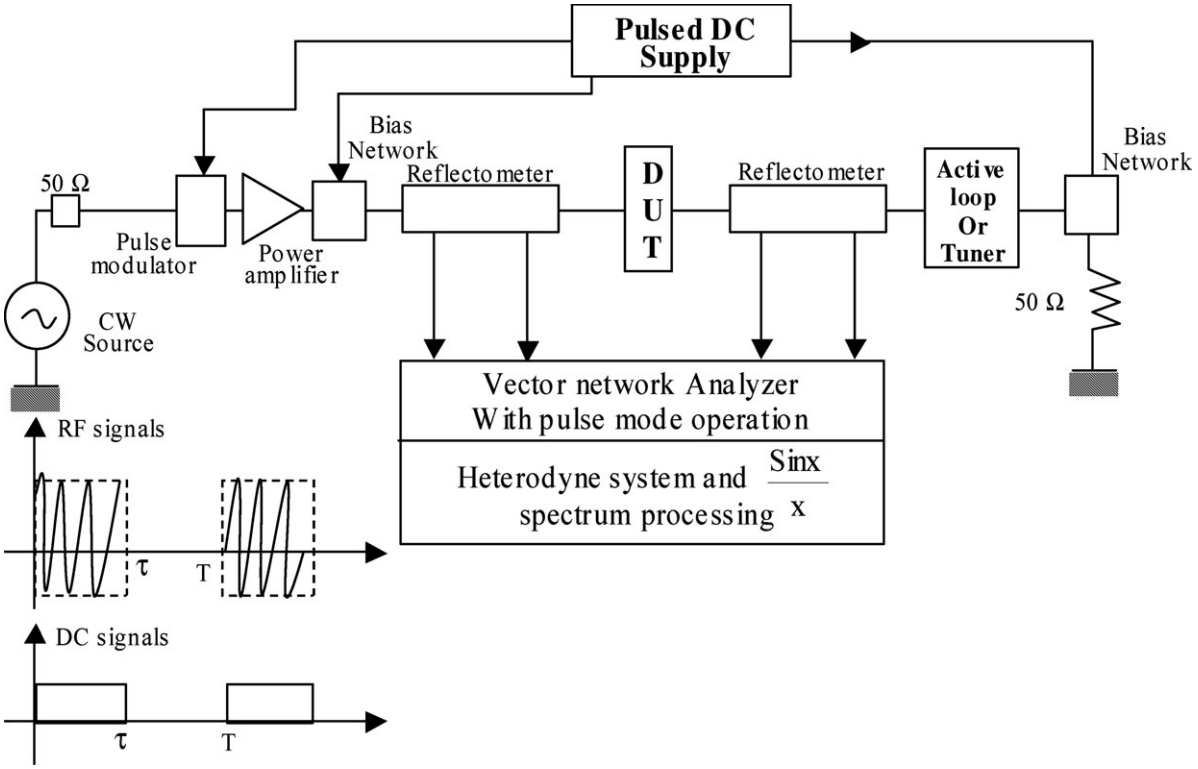

Figure 9. Pulsed load-pull set-up (DC and RF signals are synchronized duty cycle = $\frac{\tau}{T}$)

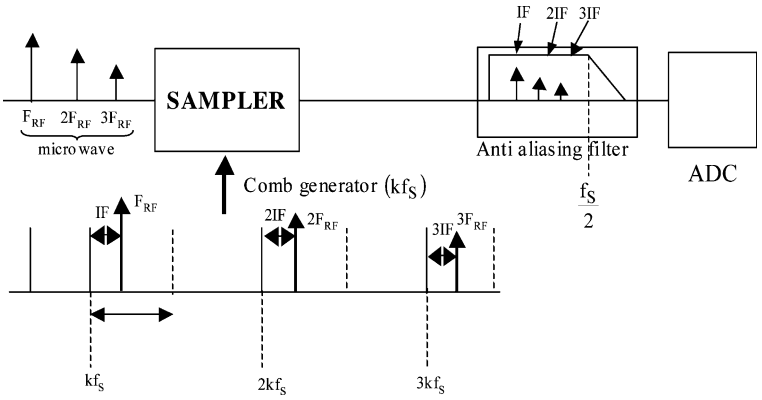

Figure 10. Principle of harmonic sub-sampling technique.

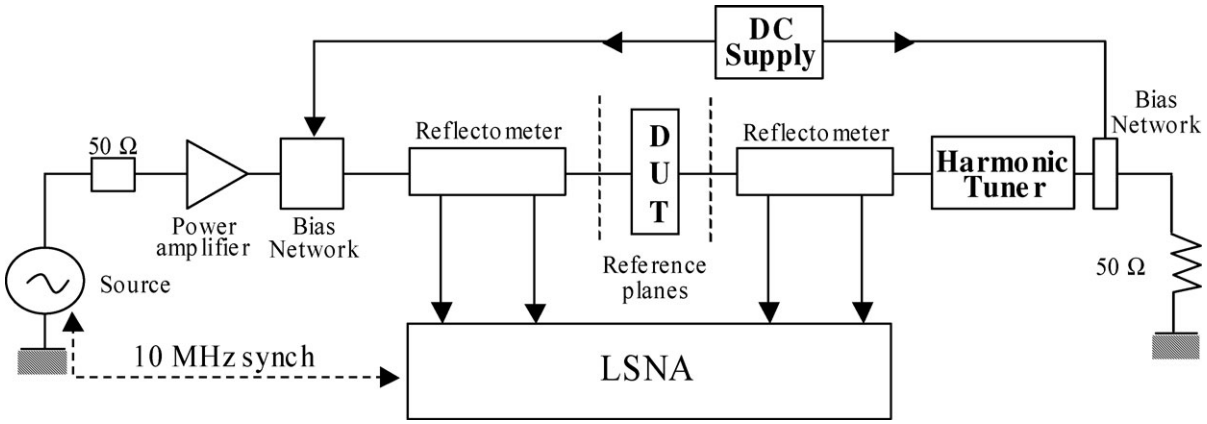

Figure 11. LSNA with load-pull set-up.

optical domains (36). The basic device is composed of two reflectors of arbitrary radius of curvature separated by a length d. At low frequencies, the dimensions of the mirror will be very large, so for this reason these devices are used essentially at very high frequencies. TEM_{plq} mode is excited in these structures, where p, l, and q are, respectively, radial, azimuthal, and axial variations of the energy which is localized in the center between the two mirrors. In a great number of applications, the TEM_{ooq} mode is used and resonant frequency of these modes are periodics along the q parameter. As in metallic cavities, the unloaded Q factor increases with the number of axial variations, and values of the Q factor greater than 10^6 are possible in millimeter-wave measurement.

Dielectric Resonators

For high frequencies the dimension of resonators excited on conventional modes becomes impractically small. A solution consists of using dielectric resonators excited on whispering gallery modes (*WGMs*), which are higher-order modes. The first advantage of this solution is the dimension of the resonators, which is approximatively 10 times bigger than resonator excited on conventional modes. The geometry of the resonators is a disk with a diameter greater than thickness, as shown in Fig. 12(c) (37, 38). So these resonators are easy to integrate in planar circuits.

Moreover, acting on these modes, energy is confined at the periphery of the dielectric resonator, and radiation losses are negligible. Thus, unloaded Q factors are very large and only limited by dielectric losses of the material used to realize the resonators.

At room temperature and using quartz material, a measured Q factor of 30,000 has been obtained at 100 GHz. Placed in a metallic cavity and at 77 K, a Q factor of 30,000,000 has been measured at 7 GHz with sapphire.

Applications to millimeter-wave measurement

In millimeter-wave devices, a large number of applications use resonators circuits. These elements are used in devices such as filters or oscillators, or for material measurements to determine complex permittivity and permeability. In both cases, it is very interesting to have a high Q factor of the resonances modes.

Filtering. Insertion losses and rejection depend on Q factor of the resonators. To realize these circuits, cylindrical metallic cavity or WGM dielectric resonators are suitable because association of several resonators is possible. At high frequencies, topologies of these structures are the same as for low-frequency devices.

Oscillator. Frequency stabilization and phase noise need a high Q value of the resonant device. For millimeter-waves, dielectric resonators excited on WGM give good results and are easy to integrate in the devices. With these modes, the original topology of oscillators can be realized by using the wave propagation effect at the periphery of the resonators, which is another property of these modes.

Dielectric Material Measurement. These resonator devices are currently used because they permit good accuracy with regard to the complex permittivity of the material. For metallic cavities or open resonators, the method consists of comparing the resonant frequency and the unloaded Q factor of the empty and loaded resonators. This method is convenient if the thickness of the material under test is smaller than the wavelength. For material with a large thickness, methods using WGM are suitable. In this case, measurements of resonance frequency and Q factor are compared with results obtained by electromagnetic simulator. These methods can be used for anisotropic dielectric or magnetic material (39).

Future Trends

The performance of millimeter-wave resonator devices is limited by the difficulty of integration of resonators in devices (in particular, for cavity or open resonators) or by losses of metallic or dielectric materials. Over the past 10 years, with the development of new dielectric materials like sapphire in the microwave domain, performances have been improved with regard to the unloaded Q factors. Unfortunately, characteristics of these materials change with temperature, and frequency stabilization is difficult to obtain without using regulating temperature devices. In the future, with technology development, we can hope to obtain material with optimum characteristics.

FREE-SPACE METHODS. INTERFEROMETRY

Waveguide loss becomes important for millimeter waves; free-space transmission has lower loss and is good for low-noise applications as well as for high-power applications (in addition, larger area of beam spread produces a lower power density). Free-space measurement is required when contact is not possible. Such is the case in radiometry for measurement of temperature and chemical composition, as well as in interferometry and in radar detection for measurement of distance, velocity, and position.

Very often for millimeter waves, the beam diameter is a relatively small number of wavelengths; thus, diffraction must be considered. A wide variety of components and systems have been developed using quasi-optical techniques, either similar to waveguide devices or derived from infrared and optical techniques (40, 41).

Quasi-Optical Techniques

Gaussian Beams. Paraxial propagation of a beam in free space is relatively simple to analyze if the transverse electric field amplitude variation has a Gaussian form:

$$\boldsymbol{E}(r)/\boldsymbol{E}(0) = \exp[-(r/w)^2]$$

where r is the distance from the axis of propagation, and w is called a "beam radius." A Gaussian beam is produced with, or focused to, a minimum size; this minimum beam radius w_0 called a "beam waist."

The feedhorn is the best coupling device between the Gaussian beam and the guided wave (Fig. 13). The best coupling (98%) is obtained with a scalar feedhorn pattern.

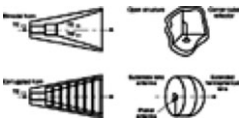

Figure 13. Devices for millimeter-wave and submillimeter-wave beam production (horn and open-structure examples).

Several types of planar antennas (patch, bow tie, traveling-wave slot) can also be used. An associated lens is used to obtain reasonable coupling efficiency. Several types of planar antennas (patch, bow tie, traveling-wave slot) can be used. An associated lens allows us to reduce the beam size and increase the coupling efficiency.

Quasi-Optical Components Used in Millimeter-Wave Measurement. Quasi-optical components provide a wide variety of functions used for millimeter measurements:

- Beam transformations require focusing elements like parabolic or ellipsoidal mirrors and lenses. To minimize the absorptive loss of lenses, low-loss dielectrics must be selected (PTFE, alumina, fused silica, etc.); and to obtain low reflection loss, a matching layer or grooves are essential, except for low-index materials.
- High Q-factor ($\gg$10,000) resonant cavities can be formed with two spherical mirrors or one spherical and one plane mirror.
- Signal filtering can be achieved by interferometers (see below) and by plate filters: Perforated conductive plates or arrays of resonant patterns are printed on a dielectric substrate.
- Polarizing grids are usual in quasi-optical systems, often used as beam splitters for a polarized signal. These grids can be formed with free-standing wires or with dielectric-supported conducting strips. Dielectric plates are also used as beam splitters and can function as hybrids (90° phase shift between reflected and transmitted beams).
- Different types of interferometers are developed from beam splitters and reflective devices: dual beam interferometers, used particularly in the FTS (Fourier Transform Spectrometers) or Fabry-Perot interferometers.

Quasi-Optical Bench. The purpose of the quasioptical bench is to create a "beam waveguide" including a sufficient measurement area. Figure 14 shows a basic bench: The measurement area is located between a signal generator and a detector equipped with free-space coupling devices (horns and lenses). The relative positions must be finely adjustable (in three rectangular directions and two or three rotating angles) while staying extremely stable. As in coaxial or waveguide measurements, generators and detectors can use frequency multipliers and heterodyne and phase-locked systems to increase the sensitivity and stability.

Free-space measurements may use a device for analog-to-coaxial calibration set parts. The methods are identical, but special care is required to (1) decrease the multiple reflections by using absorbing shields and anechoic rooms, (2) take VSWR into account, and (3) manage external (or internal) electromagnetic interferences. Another source of error and instability is atmospheric absorption, when the measuring frequency band comes over the absorption bands of an atmospheric molecule.

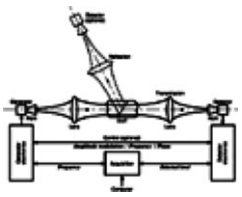

Figure 14. Quasioptical bench.

Free-Space Antenna Measurement

The antenna characteristics which have to be measured in the millimetric range are mainly radiation patterns in co- and cross-polarization. Phase center measurements of primary feeds, as well as beam efficiency, also have a great importance for reflector antenna design. Measurement techniques are much the same as at lower frequencies, but with specific difficulties and requirements (42). (See also ***Radiometry***, ***Electromagnetic field measurement***.)

Radiation Pattern Measurements. Far-field measurements must be performed outdoors if antenna dimensions are large compared with the wavelength, which generally is the case for reflector antennas at millimetric frequencies. However, atmospheric attenuation and geographic implementation become prohibitive when the far field exceeds 1 km. Compact antenna test ranges (*CATR*s) remedy this problem for medium-to-large reflector antennas in the millimetric range.

For antennas of moderate (cm) dimensions, far-field measurements can be performed indoors. Horns and printed antennas are tested in anechoic chambers. In CATRs, a local plane wave is created in a zone called the "quiet zone," by way of one or several reflectors used to collimate the beam of a smaller source. Various designs exist, ranging from the basic one with a single offset reflector to triple reflector systems, according to the required cross-polarization and spillover levels and the size of the antennas under test. Diffraction at the edges of the reflectors is less critical than in the microwave range, but reflector surfaces requirements are more stringent because the root-mean-square (*rms*) surface error should be better than 1/100 wavelength to obtain good precision on the plane wave phase. Corrugated or special multimode horns are used as sources.

Hologram CATRs are being developed. Reflectors are replaced by a hologram, with a surface accuracy requirement divided by 10. This technique is thus less expensive, but it is still very new and faces problems concerning the size of the required holograms as well as frequency bandwidth limitations (20% to 30%) and polarization difficulties.

In the near-field scanning technique, fields are measured close to the antenna under test, on either a planar, cylindrical, or spherical surface. This technique re-

quires both amplitude and phase measurements, because the sampled fields are used to calculate the radiated far-field through a near-field to far-field transformation. In the millimeter-wave domain, this technique encounters problems of time consumption and precision phase measurement.

Other Antenna Performance Measurement. The "beam efficiency measurement" is performed by measuring the power radiated within the main beam of the antenna. It is especially important for radiometer antennas, which must have very low sidelobes. It requires both radiation pattern measurements, although not with wide-angle scanning, and absolute power measurements. The "phase center position measurement" is useful only for horns used as primary sources in reflector antennas. It is performed by positioning the center of phase patterns in different planes along the axis of the horn. It requires precise phase measurements and mechanical positioners.

Quasi-Optical Measurement

Power Measurement. Most of the power detectors used in the microwave measurement (Schottky diodes for instance) still work in the millimeter-wave frequency range. Moreover, bolometers and the calorimeters also operate in this range. These devices mounted in a waveguide structure can be associated with a horn to make up a beam detector. To increase the sensitivity, synchronous detection and heterodyne conversion may be used. Absolute calibration must be performed with photoacoustic detectors (used at Brewster angle and through amplitude modulation).

Quasi-Optical Device Characteristics Measurement. A basic quasi-optical bench allows us to measure the main of millimeter-wave characteristics of a DUT inserted in the optical path: transmittance, loss and scattering by insertion, and reflection by comparison with a good reflector. Much attention must be paid to (1) the radial size of the DUT compared with the usable beam size, (2) the compensation for phase differences, and (3) the VSWR (which can be reduced by choosing an incidence angle other than zero).

For low losses, noise measurements provide a better accuracy. The equivalent noise temperature T_1 is increased to T_2 by the insertion of a DUT at the front of a low noise receiver. Giving the DUT physical temperature T_d, the loss factor L is obtained from

$$T_2 = T_d(L - 1) + LT_1(1 + \Gamma^2)$$

with $|\Gamma|^2 = [(\text{VSWR} - 1)/(\text{VSWR} + 1]^2$

Noise Measurement. In addition to classic noise measurement using a noise source (diode, gas tube) associated in this case with a horn, the common noise measurement uses two absorbing targets with two different radiant temperatures. The target with the higher temperature T_h, the "hot load," takes the place of the target with the lower temperature T_c, the "cold load," in front of the DUT. The respective output powers are P_h and P_c. With ideal targets the equivalent noise temperature of the DUT is

$$T_x = (T_h \cdot P_c - T_c \cdot P_h)/(P_h - P_c)$$

Radiometer systems must be extremely stable over long periods and linear over the whole level range. The target size must be enough to cover the whole beam. Temperature and absorption coefficients must be homogeneous over the target surface. At millimeter wavelengths, $hv < kT$, the brightness temperature is very near the physical temperature. Measurement uncertainties come from variations of the effective emissivity of the target and from the mismatch with the receiver. In addition, as a result of the standing wave effect, the total noise entering the receiver becomes frequency-dependent.

The standard ferrite-loaded foam absorbers may be used as calibration targets in the lower frequency range, but for higher frequencies the reflected power unfortunately reaches −20 dB, depending on the polarization angle. For a single polarization and when the configuration is fixed, a specially developed ridged absorber or dielectric surface at the Brewster angle acts as a quasi-perfect absorber.

To achieve good precision (<1%), a lot of specific targets have been developed from the principle of a conical hole with an angle of $<10^\circ$ to increase the number of reflections.

Other Quasi-Optical Measurements. The frequency measurement may use a down conversion by means of a millimeter mixer coupled with a local oscillator by a quasi-optical coupler (an interferometer or a simple dielectric plate). The local oscillator and the low frequency counter are phase/frequency locked on a reference ultra stable oscillator. On the other hand, wave-meters may use very-high-Q-factor cavities in quasi-optical techniques.

The measurement of the polarization of a signal usually takes advantage of the sensitivity of the detector for one electromagnetic field direction (detection diodes and rectangular waveguide mounts). To increase the accuracy or to use a nonpolarized detector, a polarized plate (grid) may be inserted (with an incident angle to decrease a possible VSWR effect). This method requires us to rotate the whole receiver or to insert a waveguide twist behind the horn (causing a calibration problem). The other solution is to use a quasi-optical polarization rotator on the optical path. This device uses three grids in transmission (43) or one grid and one reflector (44). In this way the mechanical rotation is limited to one light device, and the transition time may be very short (<10 ms). Circular polarization may be measured with a particular disposition of Martin–Puplett interferometer.

The knowledge of the insertion effects (loss and phase variations) allows us to compute the complex dielectric constant of a material. Other methods for material characteristics measurement use modifications of a cavity resonator's Q-factor.

Interferometry

The resolution of an antenna has a diffraction limit of $\approx\lambda/D$, and an interferometer increases the resolution according to the area covered by two or several connected antennas. More generally, an interferometer can be used to measure the Fourier components of a brightness distribution. Since Ryle and Hewish (45) have formulated the principle of aperture synthesis, many interferometers have been

built or are in progress (mainly for radioastronomy). The aperture may be synthesized by multiplication, physically moving of elements, or by using the rotation of the earth. As baselines are increased, the major problem in millimeter-wave measurement is the maintenance of phase stability of local oscillators; for very long baseline interferometry (*VLBI*), the local oscillators are independent and need very accurate frequency standards.

BIBLIOGRAPHY

1. Technical information available from http://www.Agilent.com, http://www.us.anritsu.com, http://www.rsd.de, http://www.vnahelp.com Online Available
2. Technical information available from Cascade Microtech Inc. [Online]. Available www: http://www.cmicro.com and Picoprobe, a GGB Industries Inc. [Online]. Available www: http://www.picoprobe.com
3. S. M. J. Liu, G. G. Boll, A new probe for W-band on-wafer measurements, *IEEE MTT-S Dig.*, 1993.
4. See application note from Cascade Microtech Inc., HP, and Picoprobe.
5. P. Crozat, J. C. Henaux, G. Vernet, Precise determination of the open circuit capacitance of coplanar probes for on-wafer automatic network analyzer measurements, *Electron. Lett.*, **27**: 1476–1478, 1991.
6. A. Davidson, K. Jones, E. Strid, LRM and LRRM calibrations with automatic determination of load inductance, *36th ARFTG Conf. Dig.*, 1990, pp. 57–63.
7. R. B. Marks, A multiline method of network analyzer calibration, *IEEE Trans. Microw. Theory Tech.*, **39**: 1205–1215, 1991.
8. G. Dambrine *et al.*, A new method for determining the F.E.T. small signal equivalent circuit, *IEEE Trans. Microw. Theory Tech.*, **36**: 1151–1159, 1988.
9. U. Stumper, Experimental investigation of mmW Six port incorporating simple waveguide structure, *IEEE Trans. Instrum. Meas.*, 469–472, 1991.
10. U. Stumper, A six port reflectometer operating at submillimeter wavelengths, *Proc. 15th Eur. Conf.*, 1985.
11. N. C. Wolker, J. E. Carrol, Simultaneous phase and amplitude measurements on opticals signals using a multiport junction, *Electron. Lett.*, **20**: 981–983, 1984.
12. G. Hjipieris, R. J. Collier, J. Griffin, A mmW six port using dielectric waveguide, *IEEE Trans. Microw. Theory Tech.*, **38**: 54–61, 1990.
13. S. A. Chahine *et al.*, A six-port reflectometer calibration using Schottky diodes operating in AC detection mode, *IEEE Trans. Instrum. Meas.*, **42**: 505–510, 1993.
14. R. J. Collier, I. M. Boese, Impedance measurements using a multistate reflectometer from 110–170 GHz, *BEMC*, 3-1, 3-4, 1996.
15. K Haddadi, H. El Aabbboui, B. Gorisse, N. Rolland, T. Lasri, A Fully In P Monolithic Integrated Millimeter-Wave Reflectometer, *36th EUMC* 2006
16. Focus Microwave Inc., An ultra wideband tuner system for load pull and noise characterization, *Microw. J.*, **38** (6): 90–94, 1995.
17. B. Bonte, C. Gaquiere, E. Boursier, G. Lemeur, Y. Crosnier An automated system for measuring power devices in Ka band. *IEEE Transaction on Microwave Theory and Techniques*, Vol. **46**, n° 1, January 1998.
18. F. M. Ghannouchi, R. G. Bosisio, Source pull/load pull oscillators measurements at microwave/MM wave frequencies, *IEEE Trans. Instrum. Meas.*, **41**: 32–35, 1992.
19. F. M. Ghannouchi Source pull measurements using reverse six port reflectometers with application to MESFET mixer design. *IEEE Trans. On Microwave, Theory and Technique* (**42**),pp 1589–1595, 1994.
20. S. Bensmida, E. Bergeault, G. I. Abib, B. Huyart Power amplifier characterization: an active load-pull system based on six-port reflectometer using complex modulated carrier. *35th European Microwave Conference*, Paris, pp 613–615, 2005
21. D. J. Williams, J. Leckey, P. J. Tasker An envelope domain analysis of measured time domain voltage and current waveforms provide for improved understanding of factors affecting linearity. *Microwave Symposium Digest, 2003—IEEE MTTs*, Vol.**2**, pp 1411–1414, June 2003.
22. F. De Groote, J. Verspecht, C. Tsironis, D. Barataud, J. P. Teyssier An improved coupling method for time domain load-pull measurements. *6th ARFTG Digest 2005*, pp 53–56.
23. F. Blache *et al.*, A novel computerized multiharmonic active load pull system for the optimization of high efficiency operating classes in power transistors, *IEEE MTT Symp.*, Orlando, FL, 1995, pp. 1037–1040.
24. G. BERGOFF and Al. Source pull and multiharmonic load-pull measurements based on six ports techniques. *IEEE Conference on Precision Electromagnetic Measurements Digest*, July 1998, pp 492–493.
25. I. Yattoun, A. Peden An improved active load-pull set-up for transistors large signal characterization in the Ka Band. *36th European Microwave Conference*, September 2006.
26. Arnaud, D. Barataud, J. M. Nebus, J. P. Teyssier, J. P. Villotte, D. Floriot" An active pulsed RF and pulsed DC load-pull system for the characterization of power transistors used in coherent radar and communication systems". *IEEE Transactions On Microwave Theory and Techniques*, Vol. **48**,pp 2625–2629, Dec. 2000.
27. J. VERSPECHT and Al. Accurate on-wafer measurement of phase and amplitude of spectral components on incident and scattered voltage wave at the signal ports of a non linear microwave device. *IEEE MTTs Symposium, Orlando*, 1995, pp 1029–1032.
28. J. VERSPECHT, K. RUSH Individual characterization of broadband sampling scopes with a nose to nose calibration procedure. *IEEE Trans. On Instrumentation Measurements*, (**43**),pp 347–354, 1994.
29. J. M. Nebus, A. Mallet, D. Barataud, F. Blache, J. P. Villotte, M. Vanden Bossche, J. Verspecht: Optimization of power added efficiency of transistors using the combination of an active harmonic load-pull set-up with a broadband vectorial nonlinear network analyzer. Invitation Workshop: New direction on nonlinear RF and microwave characterization. *IEEE MTTs 1996*, San-Francisco, TH2 B3,pp 1365–1368.
30. T. Reveyrand, A. Mallet, J. M. Nebus, M. Vanden Bossche Calibrated measurements of waveforms at internal nodes of MMICs with a LSNA and high impedance probes. *62nd ARFTG Conference Digest*, Boulder (CO), December 2003, pp 71–76.
31. D. Schreurs, K. A. Remley Use of multisine signals for efficient behavioural modelling of RF circuits with short-memory effects. *61st ARFTG Conference Digest*, Philadelphia (PA), June 13, 2003, pp 65–72.
32. P. Vael, Y. Rolain A controllable phase coherent modulated RF signal for the use with microwave network analyzer measurements. *IEEE MTT-S Digest* 1999.

33. A. Cidronali, K. C. Gupta, J. Jargon, K. A. Remley, D. De Groot, G. Manes Extraction of conversion matrices for P-HEMTs based on vectorial large-signal measurements. *IEEE MTT-S Digest*, 2003, pp 777–780.
34. J. C. McCleavy, K. Chang, Low-loss quasi-optical open resonators filters, *IEEE MTT Symp. Dig.*, 1991, pp. 313–316.
35. D. Steup, Quasioptical SMMW resonator with extremely high Q factor, *Microw. Opt. Technol. Lett.*, **8** (6): 275–279, 1995.
36. D. Cros, P. Guillon, Whispering gallery dielectric resonator modes for W-band devices, *IEEE Trans. Microw. Theory Tech.*, **38**: 1667–1674, 1990.
37. O. Di Monaco *et al.*, Mode selection for a whispering gallery mode resonator, *Electron. Lett.*, **32** (7): 669–670, 1996.
38. J. Krupka *et al.*, Study of whispering gallery modes in anisotropic single-crystal dielectric resonators, *IEEE Trans. Microw. Theory Tech.*, **42**: 56–61, 1994.
39. A. Parash, J. K. Vaid, A. Mansinch, Measurement of dielectric parameters at microwave frequencies by cavity perturbation technique, *IEEE Trans. Microw. Theory Tech.*, **27**: 791–795, 1979.
40. P. F. Goldsmith, Quasi-optical techniques at millimeter and submillimeter wave-lengths, in K. J. Button (ed.), *Infrared and Millimeter Waves*, Vol. 6, New York: Academic Press, 1982, pp. 277–343.
41. J. C. G. Lesurf, *Millimeter-wave Optics, Devices & Systems*, Bristol: Adam Hilger, 1990.
42. A. D. Olver, C. G. Parini, Millimetre wave compact antenna test ranges, *Proc. JINA 92*, Nice, 1992, pp. 121–128.
43. R. K. Garg, M. M. Pradhan, Far-infrared characteristics of multielement interference filters using different grids, *Infrared Phys.*, **18**: 292–298, 1978.
44. C. Prigent, P. Abba, M. Cheudin, A quasi-optical polarization rotator, *Int. J. Infrared Millimeter Waves*, **9** (5): 447–490, 1988.
45. M. Ryle, A. Hewish, *Monthly Notices R. Astron. Soc.*, 120–220, 1960.

GILLES DAMBRINE
PAUL CROZAT
JEAN-DOMINIQUE CROS
MAURICE GHEUDIN
BERNARD HUYART
MICHEL NEBUS
IEMN, University of Lille, Villeneuve d'Ascq, France
Paris—Sud University, Orsay, France
XLIM, Limoges University, Limoges, France
Observatoire de Paris—Meudon, Paris, France
Ecole Nationale Supérieure des Télécommunications (ENST), Paris, France